

Citation for published version:
Cunningham, C, Dhokia, V, Shokrani, A & Newman, S 2021, 'Effects of in-process LN2 cooling on the microstructure and mechanical properties of Type 316L stainless steel produced by wire arc directed energy deposition', *Materials Letters*, vol. 282, 128707. https://doi.org/10.1016/j.matlet.2020.128707

10.1016/j.matlet.2020.128707

Publication date: 2021

Document Version Peer reviewed version

Link to publication

Publisher Rights CC BY-NC-ND

# **University of Bath**

## **Alternative formats**

If you require this document in an alternative format, please contact: openaccess@bath.ac.uk

**General rights** 

Copyright and moral rights for the publications made accessible in the public portal are retained by the authors and/or other copyright owners and it is a condition of accessing publications that users recognise and abide by the legal requirements associated with these rights.

If you believe that this document breaches copyright please contact us providing details, and we will remove access to the work immediately and investigate your claim.

Download date: 08, Mar. 2023

Effects of in-process LN<sub>2</sub> cooling on the microstructure and mechanical properties of Type

316L stainless steel produced by wire arc directed energy deposition

Authors: C. R. Cunningham, V. Dhokia, A.Shokrani, S.T.Newman

Department of Mechanical Engineering, University of Bath, BA2 7AY, UK

Corresponding author: C.R.Cunningham@bath.ac.uk

Key words: 316L, additive manufacturing, anisotropy, stainless steel, WAAM

Abstract

For the first time, in-process cryogenic cooling for Wire Arc Directed Energy Deposition (DED)

and its influence on the microstructure and mechanical properties of Type 316L stainless steel

is investigated. The in-process cryogenic cooling is applied with a liquid nitrogen cryogenic jet

positioned behind the welding torch, targeting the material directly behind the melt pool during

deposition. Compared with Wire Arc DED that is conducted with a regulated interpass

temperature of 160°C, the crystallographic grain orientations of the deposit with in-process LN<sub>2</sub>

cooling were found to be significantly more random, with high numbers of equiaxed grains

generated. For the samples produced using in-process cryogenic cooling, the tensile tests

resulted in a mean Young's Modulus of 163 ± 51 GPa. This is significantly higher compared with

samples produced using interpass temperature control which resulted in a mean of  $72 \pm 27$  GPa.

BS EN 10088-1 guidance for Type 316L specifies a Young's Modulus of 200 GPa. The stiffness

improvement with in-process cooling demonstrated in this research is a significant finding for

the additive manufacture of parts by Wire Arc DED for structural applications in the architectural

and nuclear industries.

1

### 1. Introduction

The high levels of heat input in wire arc additive manufacturing often leads to microstructures with large columnar grains [1]. This can induce anisotropic and unsatisfactory material properties. Several processes and strategies exist to refine the microstructure of wire arc DED parts [2]. One such method is modification of the feedstock with inoculation [3]; however, this changes the alloy composition and can increase feedstock cost. Other methods include additional surface modification processes such as rolling, or peening applied on an intralayer or interlayer basis [4]. However, these processes typically prolong the overall part build time as parts must be cooled to a certain temperature for the cold working mechanism to be effective. In contrast, cooling-based additional processes can eliminate any interlayer dwell times, whilst also providing preferential thermal boundary conditions suitable for grain refinement. Inprocess cooling has been investigated using interlayer gas cooling [5], thermo-electric cooling [6], and immersion water-based cooling [7].

This paper investigates the use of in-process cryogenic cooling applied locally behind the weld torch with Pulse Gas Metal Arc (GMA) based Wire Arc DED. This additional process, with greater cooling capacity and increased proximity to the melt-pool has the potential to change the thermal boundary conditions more significantly than the previously explored methods and, as a consequence, impact the developed microstructures and related mechanical properties.

#### 2. Materials and methods

Thin-walls of approximately 100 mm in build height and 155 mm length in the travel direction were deposited using an ESAB Aristo 4004i welding power supply, 1 mm diameter wire and the Pulse GMA based wire arc DED process parameters of 2 m/min wire feed speed and 4.1 mm/s travel speed for each cooling condition. The configuration of equipment is presented in Fig 1a. The walls were built with a parallel path deposition strategy, with the interpass temperature

sensor (OMNI instruments, UK) shown in Fig 1b used to monitor the temperature of material at the weld start position. In-process cryogenic cooling localised to the melt-pool was implemented with liquid nitrogen (LN<sub>2</sub>) from a 3 bar pressurised, 180L Dewar (Statebourne Cryogenics Ltd, UK). The nozzle outlet as shown in Fig 1c was mounted behind the welding torch, via vacuum-jacketed pipe and moved in tandem with the electric arc. The nozzle outlet as shown in Fig 1c was positioned a few millimetres above the building height with the LN<sub>2</sub> nozzle angled to strike the deposit in the central region of the bead approximately 15 mm behind electric arc. This configuration ensured that the LN<sub>2</sub> and the expanding gaseous N<sub>2</sub> struck the surface of the deposit without expansion of gaseous N<sub>2</sub> disrupting the arc.

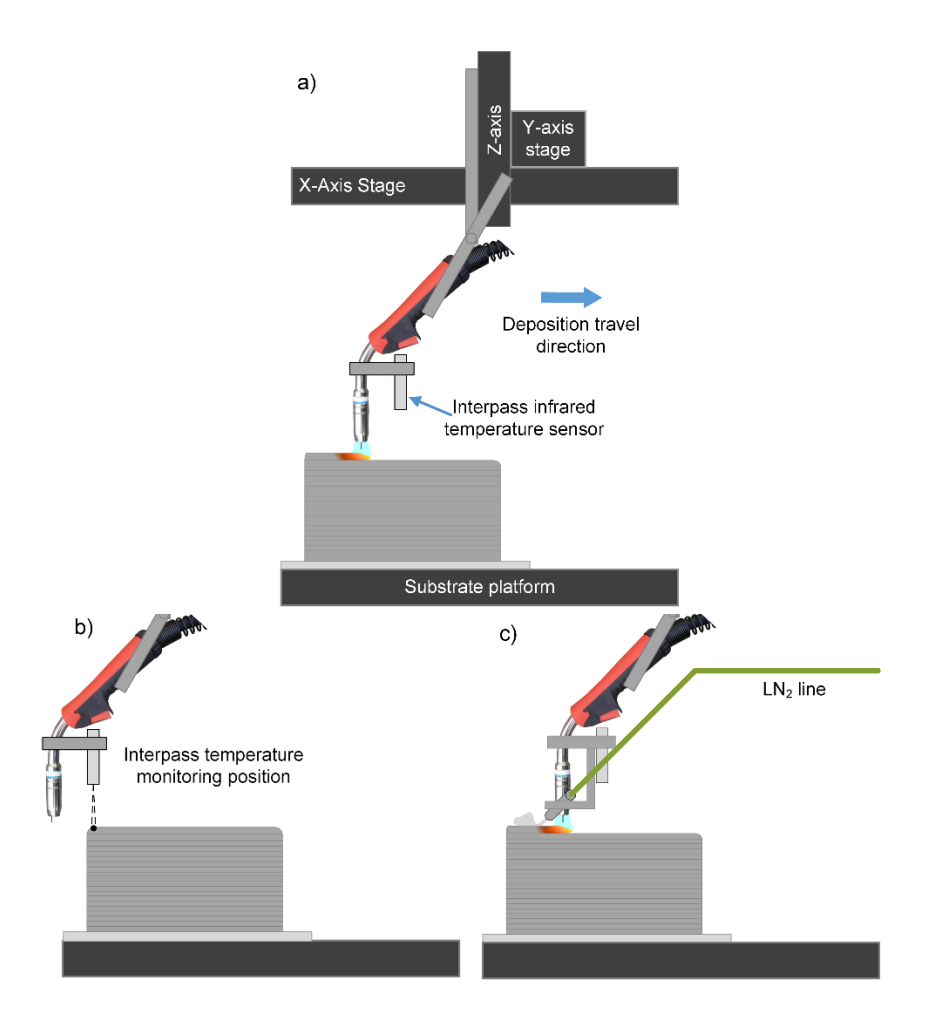


Figure 1 Schematic of the configuration of the wire arc DED equipment for the  $160^{\circ}$ C interpass temperature experiment a) during deposition b) in the interpass temperature monitoring position at the deposition start point and c) the in-process cryogenic cooling set up during deposition showing the  $LN_2$  jet angled behind the melt-pool.

Following deposition, the walls were sectioned, and samples extracted for Electron Back Scatter Diffraction (EBSD) analysis and tensile testing as shown in Fig 2. Standard metallographic preparation procedures as detailed in ASTM E3 were followed [8], and the dimensions of the tensile samples were in accordance with ASTM E8/E8M [9] with a 3.2 mm sample thickness. Uniaxial tensile tests were performed at room temperature using an Instron 3369, 50 kN load cell with an Instron 2630-106 clip gauge extensometer to record strain to estimate Young's Modulus (E). An extension rate of  $7 \times 10^{-5}$  was used in the elastic deformation region. For imaging of the sample texture, a central region of the middle section shown in Fig 2 was scanned with a JEOL JSM-IT500 InTouchScope<sup>TM</sup> with EBSD capability in the YZ plane. Specimens were aligned such that the build direction points upwards, and the SEM images were taken at a similar height in the build direction to maintain consistency. The 100x and 2000x magnification images covered an area of 1250 by 971  $\mu$ m (step size 4.00  $\mu$ m) and 62 by 48  $\mu$ m (step size 90 nm) respectively. TSL OIM Analysis<sup>TM</sup> 8 software was used to analyse the results of the EBSD scans.

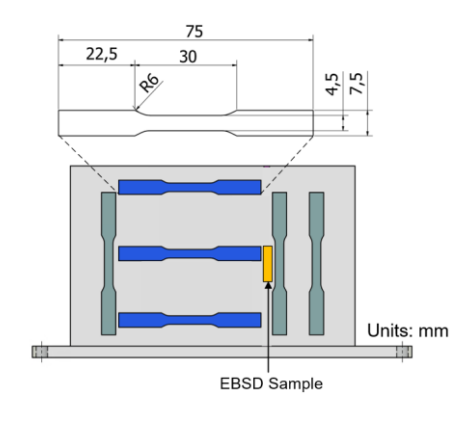


Figure 2 Schematic showing the tensile specimen and EBSD sample extraction locations.

### 3. Results and Discussion

EBSD inverse pole figures (IPFs) highlighting grain orientation are presented in Fig 3. The interpass temperature control sample contains large columnar grains aligned to the build direction as shown in Fig 3a and b and are typical of those produced using Wire Arc DED [10]. In contrast, the in-process cooling produced sample shown in Fig. 3c, contains grains of reduced size and texture with a feathered morphology, which is more typical of microstructures reported for powder-laser DED [11]. Whilst Fig 3c covers a smaller area, Fig 3a shows distinct columnar grains, with no region containing diversity of grain orientations shown by the in-process cooled sample (Fig 3c). This indicates a fundamental localised change in grain nucleation and growth. This can be attributed to the change in direction of maximum thermal gradient, interrupting the dominant grain growth along the <100> easy growth direction. Rapid cooling of the melt-pool also promotes nucleation ahead of the solidification front and hinders grain growth [12]. For both processing conditions, the grains exhibited notable mosaicity with slight fluctuations in the colouration of IPF maps. This is representative of strain within the samples accommodated by dislocations and crystallographic misorientation [13].

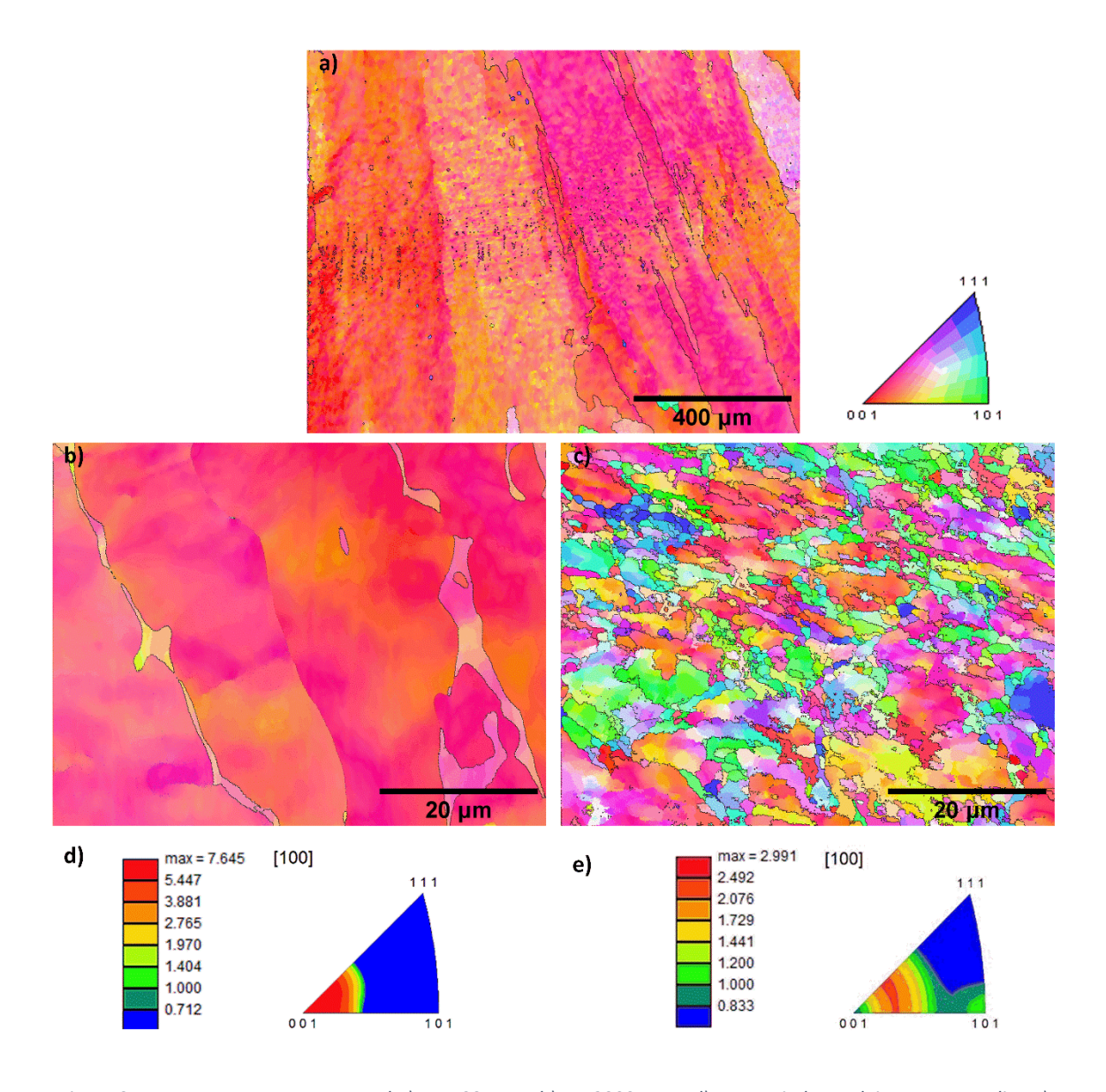


Figure 3 Interpass temperature control a) IPF 100x mag b) IPF 2000x mag d) texture index and, in-process cooling c)

IPF x2000 mag e) texture index. The reference direction for all IPF maps is the build direction (BD).

The tensile testing allowed the yield strength and Young's Modulus to be determined as shown in Fig. 4. It can be seen that the yield strength increases from 288  $\pm$  22 MPa to 314  $\pm$  16 MPa with the application of in-process cooling, whereas the elongation varied only marginally from 41.1%  $\pm$  3.9% and 42.1%  $\pm$  5.2% respectively. The mean E of the cooled specimens (163  $\pm$  51 GPa) is significantly higher than for the specimens built with interpass temperature control (72  $\pm$  27 GPa). As E varies with crystallographic orientation, it can be calculated using the elastic constants  $C_{11}$ ,  $C_{12}$  and  $C_{44}$  provided by Ledbetter for mono-crystalline Type 316 [14]. This

estimates  $E_{001} = 102$  GPa,  $E_{101} = 196$  GPa, and  $E_{111} = 280$  GPa. As the cooled sample contains more randomly orientated grains, E is closer to that expected of wrought plate material (200 GPa) [15] providing additional stiffness compared to the interpass temperature control sample, which is strongly aligned to the <100> build direction. However, E values in the <100> aligned sample were below the monocrystalline estimate of 102 GPa. Possible causes for this include the dispersion of fine oxide particles and high dislocation density prior to deformation caused by the process-induced residual stresses. The greater scatter in E of the cryogenic samples can be attributed to the stochastic grain orientation at the necking point combined with the remaining large grains. The scatter in comparison to wrought material suggests that Wire Arc DED samples still retain a heterogeneous microstructure, despite the grain refinement achieved in the inprocess cooling case.

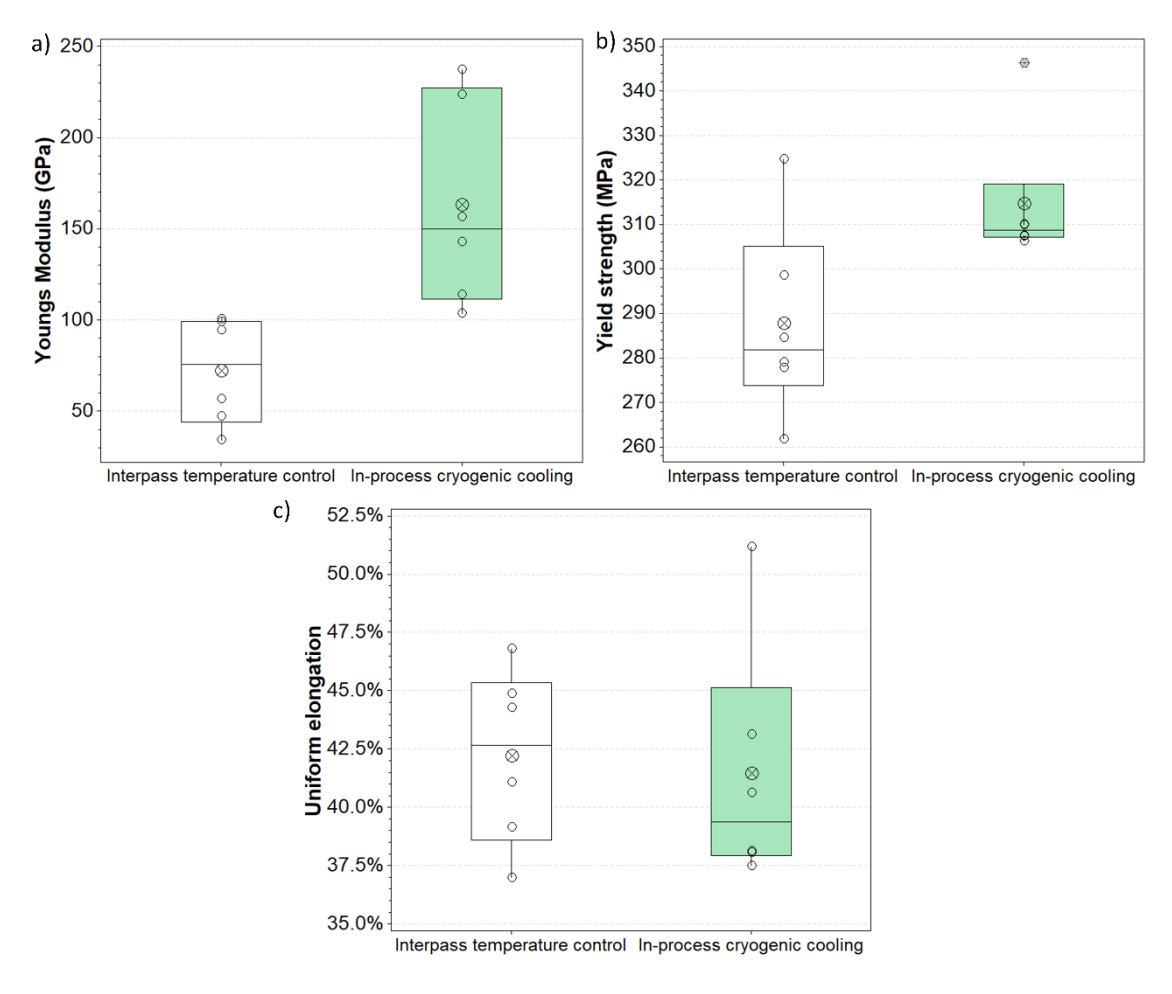


Figure 4 Interpass temperature control and in-process cryogenic cooling a) E b) yield strength c) uniform elongation

### 4. Conclusions

In this paper, the grain structure of Type 316L stainless steel produced by Wire Arc DED was analysed under the conditions of interpass temperature control and in-process cryogenic cooling. The metallurgical and mechanical properties were investigated with the conclusions summarized as follows:

- In-process cryogenic cooling can be used to modify the as-built microstructure of wire arc DED parts. The cooled samples displayed finer, equiaxed grains of size and texture that was more typical of Laser-DED than a Wire Arc DED process.
- A moderate increase in yield strength from 288  $\pm$  22 MPa to 314  $\pm$  16 MPa occurs with additional in-process cooling.
- In-process cryogenic cooling increased E by 126% compared to the use of interpass temperature control by reducing the texture of grains aligned to the <100> build direction. The increase in stiffness with in-process cooling is a significant finding for Wire Arc DED parts for structural architectural and nuclear applications.

#### **Acknowledgements**

The authors would like to acknowledge support from Engineering and Physical Sciences Research Council Case Studentship (No. 1780168), and also thank Renishaw plc for their support and assistance with EBSD imaging.

### References

[1] S.W. Williams, F. Martina, A.C. Addison, J. Ding, G. Pardal, P. Colegrove, Wire + Arc Additive Manufacturing, Materials Science and Technology 32(7) (2016) 641-647.

- [2] C.R. Cunningham, J.M. Flynn, A. Shokrani, V. Dhokia, S.T. Newman, Invited review article: Strategies and processes for high quality wire arc additive manufacturing, Additive Manufacturing 22 (2018) 672-686.
- [3] M. Mizumoto, S. Sasaki, T. Ohgai, A. Kagawa, Development of new additive for grain refinement of austenitic stainless steel, International Journal of Cast Metals Research 21(1-4) (2013) 49-55.
- [4] P.A. Colegrove, H.E. Coules, J. Fairman, F. Martina, T. Kashoob, H. Mamash, L.D. Cozzolino, Microstructure and residual stress improvement in wire and arc additively manufactured parts through high-pressure rolling, Journal of Materials Processing Technology 213(10) (2013) 1782-1791.
- [5] P. Henckell, K. Günther, Y. Ali, J.P. Bergmann, J. Scholz, P. Forêt, The Influence of Gas Cooling in Context of Wire Arc Additive Manufacturing—A Novel Strategy of Affecting Grain Structure and Size, TMS 2017 146th Annual Meeting & Exhibition Supplemental Proceedings (2017) 147-156.
- [6] F. Li, S.J. Chen, J.B. Shi, Y. Zhao, H.Y. Tian, Thermoelectric Cooling-Aided Bead Geometry Regulation in Wire and Arc-Based Additive Manufacturing of Thin-Walled Structures, Appl Sci-Basel 8(2) (2018) 1-12.
- [7] L.J. da Silva, D.M. Souza, D.B. de Araújo, R.P. Reis, A. Scotti, Concept and validation of an active cooling technique to mitigate heat accumulation in WAAM, The International Journal of Advanced Manufacturing Technology 107(5-6) (2020) 2513-2523.
- [8] ASTM E3, Standard Guide for Preparation of Metallographic Specimens, 2011.
- [9] ASTM E8/E8M, Standard Test Methods for Tension Testing of Metallic Materials, 2013.

- [10] V. Chakkravarthy, S. Jerome, Printability of multiwalled SS 316L by wire arc additive manufacturing route with tunable texture, Materials Letters 260(126981) (2020) 1-4.
- [11] Z. Wang, T.A. Palmer, A.M. Beese, Effect of processing parameters on microstructure and tensile properties of austenitic stainless steel 304L made by directed energy deposition additive manufacturing, Acta Materialia 110 (2016) 226-235.
- [12] J.P. Oliveira, T.G. Santos, R.M. Miranda, Revisiting fundamental welding concepts to improve additive manufacturing: From theory to practice, Progress in Materials Science 107 (2020).
- [13] Z. Yanushkevich, S.V. Dobatkin, A. Belyakov, R. Kaibyshev, Hall-Petch relationship for austenitic stainless steels processed by large strain warm rolling, Acta Materialia 136 (2017) 39-48.
- [14] H. Ledbetter, Austenitic-steel elastic constants, Austenitic steels at low temperatures, Springer1983, pp. 83-103.
- [15] BS EN 10088-1, Stainless steels. Part 1: List of stainless steels, (2014).